Water purification in a solar reactor incorporating TiO_2 coated mesh structures

El-Kalliny, Amer S.; Rivandi, Alireza H.; Uzun, Sibel; Van Ommen, J. Ruud; Nugteren, Henk W.; Rietveld, Luuk C.; Appel, Peter W.

DOI
10.2166/ws.2019.052

Publication date
2019

Document Version
Final published version

Published in
Water Science and Technology: Water Supply

Citation (APA)
El-Kalliny, A. S., Rivandi, A. H., Uzun, S., Van Ommen, J. R., Nugteren, H. W., Rietveld, L. C., & Appel, P. W. (2019). Water purification in a solar reactor incorporating TiO_2 coated mesh structures. *Water Science and Technology: Water Supply*, *19*(6), 1718-1725. https://doi.org/10.2166/ws.2019.052

Water purification in a solar reactor incorporating TiO_2 coated mesh structures

Amer S. El-Kalliny, Alireza H. Rivandi, Sibel Uzun, J. Ruud van Ommen, Henk W. Nugteren, Luuk C. Rietveld and Peter W. Appel

ABSTRACT

The rate of photocatalytic oxidation of contaminants in drinking water using an immobilized catalyst can be increased by properly designing the catalyst structure. By creating a solar reactor in which meshes coated with TiO_2 were stacked, we demonstrated that degradation of humic acids with four superimposed stainless steel meshes was up to 3.4 times faster than in a single plate flat-bed reactor. Incorporation of TiO_2 coated mesh structures resulted in a high specific photocatalytically active surface area with sufficient light penetration in the reactor, while the coated area for one mesh was 0.77 m^2 per m^2 projected area. This brought the photocatalytic efficiency of such reactors closer to that of dispersed-phase reactors, but without the complex separation of the very fine TiO_2 particles from the treated water.

Key words | humic acid, immobilized TiO_2, mesh structure, photocatalysis, solar reactor, water purification

Amer S. El-Kalliny (corresponding author)
Alireza H. Rivandi
Sibel Uzun
J. Ruud van Ommen
Henk W. Nugteren
Peter W. Appel
Product and Process Engineering, Department of Chemical Engineering, Faculty of Applied Sciences,
Delft University of Technology,
Van der Maasweg 9 (Building 58), 2629 HZ Delft,
The Netherlands
E-mail: *kalliny78@hotmail.com*; *as.el-kalliny@nrc.sci.eg*

Amer S. El-Kalliny
Luuk C. Rietveld
Sanitary Engineering, Faculty of Civil Engineering and Geosciences,
Delft University of Technology,
Stevinweg 1, 2628 CN Delft,
The Netherlands

Amer S. El-Kalliny
Water Pollution Research Department,
National Research Centre,
33 El Buhouth St., Dokki, 12622 Giza,
Egypt

Sibel Uzun
Head of Consumer Safety and Public Health Laboratories, General Directorate of Public Health, Turkish Ministry of Health,
Adnan Saygun Street, No. 55, Sıhhıye, Cankaya,
Ankara,
Turkey

INTRODUCTION

Heterogeneous solar photocatalysis uses solar UV light in the range between 300 nm and 400 nm to photo-excite the catalyst in contact with water and in the presence of oxygen (Malato *et al.* 2009) to generate hydroxyl radicals (˙OH). TiO_2 is the most-used photocatalyst because of its biological and chemical inertness, photo-stability, availability, and non-toxicity (McCullagh *et al.* 2011). The largest exposed active catalyst surface area, relative to the reactor volume, can be obtained in a so-called dispersed-phase reactor. However, a complex and expensive separation step is required to remove the fine catalyst particles from the water. This can be avoided by using immobilized photocatalyst reactors (Feitz *et al.* 2000; Malato *et al.* 2009; McCullagh *et al.* 2011). For efficient contaminant degradation such reactors require a large reactor surface with low throughput because of their low catalyst surface to reactor volume ratio. The degradation potential can be increased by changing the configuration of such reactors. Zhang *et al.* (2004) reported that the rate of

doi: 10.2166/ws.2019.052

degradation with a corrugated plate was a factor 1.5 faster than with the flat-plate for the same exposed reactor area. More complex configurations can be used to increase even further the catalyst surface to reactor volume ratio. However, although the catalyst surface to reactor volume ratio may increase, light penetration in the reactor can then become a limiting factor (Feitz *et al.* 2000; Dijkstra *et al.* 2001).

TiO_2 coatings were successfully applied on various materials of different surface areas such as ordinary glass and borosilicate glass (Parra *et al.* 2004; Fujishima *et al.* 2008; Zhang *et al.* 2012), cellulose fibres (Goetz *et al.* 2009), and stainless steel (Yanagida *et al.* 2006). To optimize the active catalyst surface to reactor volume ratio as well as light penetration and light distribution, a novel reactor was developed containing a stack of TiO_2 coated meshes (El-Kalliny *et al.* 2014). Stainless steel woven meshes were used as catalyst support material and TiO_2 coatings were applied by electrophoretic deposition (EPD) using a commercial sol gel (O5100) as a stable suspended electrolyte. In this paper, the TiO_2 coated mesh reactor was used to study the adsorption and solar photocatalytic degradation efficiency of humic acids (HA) as a model compound for surface water contaminants. The performance of the catalyst structure was investigated at different scales, including a batch system in a beaker and a recirculating flow fixed-bed reactor. Results were compared with those obtained with a similarly coated flat-plate reactor of the same size.

EXPERIMENTAL METHODS

Preparation of the immobilized TiO_2 catalyst

Immobilization of the TiO_2 photocatalyst on grade 304 stainless steel woven meshes and flat plates was done using the EPD technique described in El-Kalliny *et al.* (2014). Meshes had a wire diameter of 0.355 mm and an aperture diameter of 0.915 mm, resulting in an open area of 52%. Flat plates were 2 mm thick and had the same dimensions as the rectangular mesh sheets (32 cm × 19 cm).

Fixed-bed reactor and photocatalytic activity evaluation

The batch experiments with small circular meshes (ø 5.5 cm) were carried out in 250 mL Pyrex glass beakers (internal diameter 7 cm) using a magnetic stirrer (IKA, RT15) with a stirring rate of 550 rpm. The meshes were placed on top of each other and separated by 2-mm-thick silicone rubber rings. The temperature was kept at 32 ± 1 °C by using a recirculation cooler (Julabo, FL300). This temperature is a simulation for the temperature of the system subjected to solar light. Working solutions of HA were prepared from a 1,000 $mg \cdot L^{-1}$ stock solution of HA sodium salt (Sigma Aldrich). The HA sodium salt was dissolved in aerated deionized water and filtered through a 0.45 μm syringe-driven filter unit (Millex) to remove suspended solids (0.03 $g \cdot L^{-1}$).

The schematic view of the fixed-bed photocatalytic reactor is presented in the Supplementary Data (Figure S1), available with the online version of this paper. The body of the reactor was made of Perspex and the cover was 4-mm-thick borosilicate glass. UV solar light (300–400 nm) transmission of this cover, measured by Xenocal UV-sensor (Atlas), was 92.9%. Four mesh layers (32 cm × 19 cm) were placed in the reactor, separated by 2-mm-thick silicone rubber spacers. Water recirculated and entered into the reactor from the short side (19 cm width) by a peristaltic pump (Minipuls 3, Gilson) with a maximum flow rate of 200 $mL \cdot min^{-1}$, corresponding to a hydraulic retention time through the reactor of 3.25 min. These conditions showed that there were no dead zones in the reactor with a good mixing as clarified by the color injection method. This method showed that mixing occurred within 10 s, which is a very short time compared with the reaction retention time of about 1 hour. Mixing of outlet water was done in a separate container by a magnetic stirrer. In the flat plate reactor experiment, the flat plate of 32 cm × 19 cm coated with TiO_2 was placed instead of mesh layers. The chamber of a SUNTEST XXL+ (Atlas) equipped with three Xenon lamps irradiating solar light (65 $J \cdot m^{-2} \cdot s^{-1}$ intensity in the range of 300–400 nm) was used for both systems.

Adsorption experiments of HA in the dark

Before HA degradation experiments under solar light could be done, adsorption experiments of HA on TiO_2 coated films over stainless steel woven meshes were carried out in the dark. The adsorption experiments were carried out with 100 mL and 2 L of HA solution of the desired concentrations in batch and in recirculating flow fixed-bed systems,

respectively, at constant temperature 32 °C ±1 °C. The adsorbed amount of HA (q_t, mg·m^{-2}) on the coated meshes was determined by:

$$q_t = \frac{(C_o - C_t)V}{A_S} \quad (1)$$

where C_o (mg·L^{-1}) is the concentration of HA at t_0, C_t (mg·L^{-1}) is the concentration of HA at t_t, V (L) is the volume of the HA solution, and A_S (m^2) is the surface area of the stainless steel woven mesh coated by the photocatalyst. A_S is half the value of the total surface area of the mesh (A_{Mesh}) as the TiO_2 film was coated on one side of the mesh which was facing the anode in the EPD process. Hence:

$$A_S = \frac{1}{2}A_{Mesh} = \frac{1}{2}L\pi D \quad (2)$$

where L (m) is the total length of the wire from which the mesh is made and D (m) is the diameter of the wire. No corrections for the wire diameter due to the coating were carried out as it was small compared with the diameter of the virgin wire. The length of the wire was determined by:

$$L = \frac{4W}{\rho\pi D^2} \quad (3)$$

where W (kg) is the weight of the wire mesh and ρ is the density of the stainless steel (7,977 kg·m^{-3}). By weighing a mesh, the surface area of that mesh was calculated knowing its wire diameter (0.355 mm according to the manufacturer). The 5.8 cm diameter disk used in the batch experiments weighed 2.88 g, so its coated surface area was 20.3 cm^2 for a projected area A_P of 26.4 cm^2. The coated area was thus 0.77 m^2 per m^2 projected area.

Because of the grid structure of the mesh, there was wire overlap at the contact points. From basic geometrical considerations it can be calculated that for the given wire diameter and mesh aperture the overlap was 16.25% of the total wire surface. The exposed coated surface area A_S was therefore corrected accordingly.

The adsorption experiments were carried out in the dark for different starting concentrations in the range of 6 mg·L^{-1} to 14 mg·L^{-1}. Assuming that the adsorption kinetics of HA onto the TiO_2 film on the meshes follows a pseudo-first-order Lagergren kinetic model, the amount of HA adsorbed at equilibrium (q_e) can be obtained from curve-fitting of the data to the equation of that model (Qiu *et al.* 2009; Zhao *et al.* 2010):

$$q_t = q_e(1 - e^{-k_1 t}) \quad (4)$$

where q_e (mg·m^{-2}) and q_t (mg·m^{-2}) are the amounts of HA adsorbed at equilibrium and at time t (min), respectively, and k_1 (min^{-1}) is the pseudo-first-order rate constant. The adsorbed amount at equilibrium, q_e (mg·m^{-2}), can be obtained through the empirical equation proposed by Freundlich (Zhao *et al.* 2010):

$$q_e = K_f C_e^n \quad (5)$$

where K_f (L·m^{-2}, in case of $n = 1$) is the Freundlich isotherm constant and is a measure of adsorptive capacity, and n determines the intensity of adsorption.

Precise experimental determination of both q_e and C_e is difficult because of mass conservation; both are related to the initial concentration of HA in the solution (C_0). By combining Equations (4) and (5) and substituting C_0 for C_e, with an assumption that q_e is C_0-dependent in order to simplify the calculations, the amount of HA adsorbed q_t at t_t can be obtained by the following equation:

$$q_t = K_f C_0^n(1 - e^{-k_1 t}) \quad (6)$$

Analytical methods

The HA concentration was determined by the UV absorption at 254 nm, which is representative of the aromatic moieties. This was done with a Hach Lange DR 5,000 spectrophotometer as described in El-Kalliny *et al.* (2014).

Solar radiation evaluation

The intensity of the UV solar light (300–400 nm) was measured with a Xenocal UV-sensor with a resolution of 0.1 J·m^{-2}·s^{-1}. The exposed energy $Q_{UV,N}$ (kJ·L^{-1}) is the

total radiation energy absorbed per unit volume in the reactor from the beginning of an experiment up to a given time (Bandala *et al.* 2002; Sichel *et al.* 2007) and it was determined by Malato *et al.* (1999) as:

$$Q_{UV,N} = Q_{UV,N-1} + \Delta t_n I_N \frac{A_P}{V} \quad (7)$$

with

$$\Delta t_n = t_n - t_{n-1} \quad (8)$$

where t_n(s) is the experimental time for each sample, I_N (kJ·m^{-2}·s^{-1}) is the intensity of solar $UV_{300\text{-}400\ nm}$ irradiation projected on top of a mesh layer during the time interval t_n, A_P (m^2) is the projected area for the mesh layer, N is the number of the mesh layers, and V (L) is the reactor volume. In the case of a first-order reaction, the reaction rate is expressed in units of mg·kJ^{-1} of UV irradiated on the catalyst surface, as the exposed energy was used instead of time to describe the process.

I_N, A_P, and V were taken into account by calculating $Q_{UV,N}$ for each mesh and the total absorbed energy in the reactor was obtained by adding the values of all the mesh layers. I_N in $UV_{300\text{-}400\ nm}$ on top of the N^{th} mesh (N is an integer ≥ 1) for the small-scale batch system was determined by El-Kalliny *et al.* (2014):

$$I_N = I_o(1-r)^{(N-1)} e^{-\varepsilon CNd} \quad (9)$$

where I_o (kJ·m^{-2}·s^{-1}) is the intensity of light on top of the water surface, r (dimensionless) is the fraction of light absorbed by each mesh, assuming that there is no back or forth reflection from the mesh layers (El-Kalliny *et al.* 2014), ε is the extinction coefficient of HA at λ from 300 nm to 400 nm ($\varepsilon_{HA,254\ nm} = 0.0717$ L·mg^{-1}·cm^{-1}), C (mg·L^{-1}) is the HA concentration, and d (cm) is the separation distance between the meshes. The transmission of $UV_{300\text{-}400\ nm}$ through 1 cm of HA (10 mg.L^{-1}), measured by the Xenocal UV-sensor, is equal to 0.77 and consequently the $\varepsilon_{HA,300\text{-}400\ nm}$ is equal to 0.027 L·mg^{-1}·cm^{-1}. Through Equation (9), the HA light absorption is taken into account, where the HA concentration is homogeneously distributed over the reactor (El-Kalliny *et al.* 2014).

For the large-scale fixed-bed reactor, the separators were taken into account and the intensity of solar $UV_{300\text{-}400\ nm}$ I_N (kJ·m^{-2}·s^{-1}) on top of the N^{th} mesh was determined by:

$$I_N = I_o(1-r)^{(N-1)} \left(\frac{A_T - A_{Sep}}{A_T}\right) e^{-\varepsilon CNd} \quad (10)$$

where A_T (m^2) is the total area of the mesh layer, and A_{Sep}(m^2) is the area of the separator that blocks the light.

The applicability of the Langmuir–Hinshelwood (LH) model gives an interpretation for the mechanism of the photocatalytic degradation of HA using coated meshes. The reaction rate in exposed energy Q is obtained by using the LH expression given by Kumar *et al.* (2008):

$$r = \frac{-dC}{dQ} = \frac{k_r K_{LH} C}{1 + K_{LH} C} \quad (11)$$

where k_r is the rate constant of photochemical reaction, and K_{LH} is the adsorption coefficient of HA onto the catalyst during the irradiation period. If the LH obeys pseudo-first-order kinetics, then r and k_r are in mg·kJ^{-1} and K_{LH} is in L·mg^{-1}. The reaction rate r is represented as a function of the initial concentration of HA (C_o) as follows:

$$r_o = k_{app} C_o = \frac{k_r K_{LH} C_o}{1 + K_{LH} C_o} \quad (12)$$

The parameters k_r and K_{LH} were predicted by linearizing Equation (12) as follows:

$$\frac{1}{k_{app} C_o} = \frac{1}{k_r} + \frac{1}{k_r K_{LH} C_o} \quad (13)$$

RESULTS AND DISCUSSION

Adsorption of HA on coated meshes

Figure 1 shows q_t (mg·m^{-2}) as a function of contact time for the small and large mesh structures in the batch system and in the recirculating flow fixed-bed reactor, respectively. The data show a strong increase in q_t during the first 20 minutes, levelling off thereafter to a saturation value at

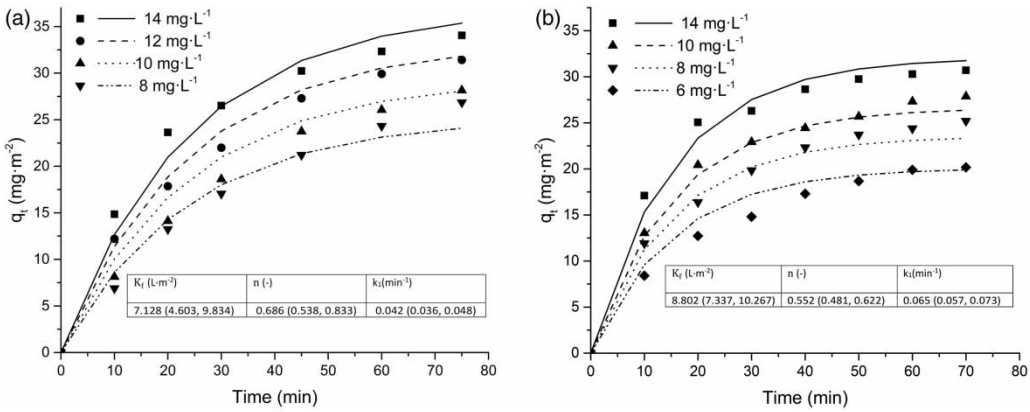

Figure 1 | Adsorption kinetics of HA onto: (a) small coated meshes in the batch reactor and (b) large coated meshes in the recirculating flow fixed-bed reactor for initial concentration C_o varying between 6 and 14 mg·L^{-1}. The lines are obtained by curve-fitting of the measured data according to Equation (6).

equilibrium. Figure 1 shows that the adsorption capacity increased with increasing C_o. This is an indication of the presence of sufficient active sites per unit volume that can acquire and adsorb HA molecules with increasing C_o. The values of K_f, n, and k_1 (from Equation (6)) were obtained by least-square-fitting of the experimental measurements and the resulting curves are drawn for different C_0 in Figure 1. The good fit shows that the adsorption kinetics of HA onto the TiO_2 film coated on the meshes are well-described by the combination of the pseudo-first-order kinetic model and the Freundlich adsorption model (Equation (6)). Therefore, probably a multilayer of adsorbed molecules was formed on the catalyst surface and saturated the adsorption sites. The values of the constants and the corresponding 95% confidence level intervals are inserted in Figure 1. The fit has R^2 of 0.964 and 0.961 with the root-mean-square deviation equal to 1.43 and 1.17 for the small meshes and the large meshes, respectively. The K_f for the recirculating flow fixed-bed reactor was slightly higher than for the batch system. This reflected a difference range of 7%–14% of calculated q_e values (Supplementary Data, Table S1, available with the online version of this paper). It was found that the calculated q_e (via Equation (5)) for small meshes ranged from 44.12 to 30.05 mg·m^{-2} for small meshes and ranged from 37.78 to 27.74 mg·m^{-2} for large meshes with C_o values of 14–8 mg·L^{-1}. The similarity between the two systems in the behaviour of HA adsorption over the meshes suggests that up-scaling of the mesh structure is feasible. Further, the higher value of the kinetic constant k_1 suggests that there were no mass transfer limitations in the recirculating flow fixed-bed reactor compared with the well-stirred batch system.

Solar photocatalytic degradation of HA

Before starting photocatalytic degradation experiments, the systems were preconditioned for 2 h in the dark to attain adsorption equilibrium. When exposure to solar light started, the HA concentration was equal to the C_e. Therefore, in Figure 2, the decrease of HA concentration due to exposed solar energy Q (in kJ·L^{-1}) is given as C/C_e for different C_0 values. An additional photolysis experiment was done in the batch reactor by irradiating a HA solution of 10 mg·L^{-1} without any photocatalyst present. The results in Figure 2(a) show that no noticeable degradation of HA occurred up to 12.5 kJ·L^{-1} of solar energy irradiation without the catalyst. However, when applying the small coated meshes, HA concentrations were reduced to less than half of those when solar irradiation started. By using a flat plate in the fixed bed reactor at an initial HA concentration of 10 mg·L^{-1} the solar photocatalytic degradation of HA was 3.4 times lower than in the case of the coated mesh structure at the same exposed energy (Figure 2(b)). Even though the light intensity was not homogeneously distributed over the expanded surface area (A_S for four coated meshes was increased from 1 m^2 to 3 m^2, see above), the attenuation factor was still higher than 3, indicating that a more spatial distribution of light over the surface was beneficial. Not only were more active sites of TiO_2 photocatalyst available on the mesh structure than on the

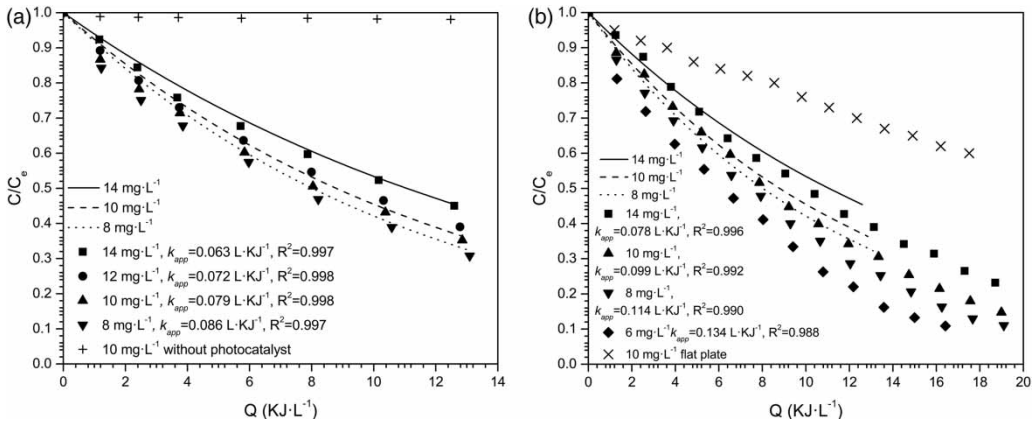

Figure 2 | (a) Solar photolysis of HA (10 mg.L^{-1}) and solar photocatalytic degradation of HA with different initial concentrations (C_0) using coated meshes in the batch reactor; (b) solar photocatalytic degradation of HA with different initial concentrations (C_0) using coated meshes and a flat plate in the fixed-bed solar photocatalytic reactor. Lines represent the pseudo-first-order kinetics of HA degradation for small meshes. These lines are presented also in (b) to show the extent of deviations between the two systems.

flat plate for the same volume of water, but these sites were also more efficient due to better light distribution. Fujishima *et al.* (2008) already showed that the catalyst efficiency increases by immobilization on a large surface area support, due to an increase in the surface-area-to-volume ratio (Fujishima *et al.* 2008). That the mesh structure allowed a high light penetration and distribution in the reactor was reported earlier (El-Kalliny *et al.* 2014), but now it is also shown that this translates into increased photodegradation of HA.

In order to investigate the dependence of photocatalytic degradation on the adsorption step by checking the applicability of the LH model, it is essential to calculate the apparent rate constants (k_{app}) for the removal of HA for different initial HA concentrations (Equation (12)). The relations between ln(C) and the exposed energy (Q), including light absorption, resulted in straight lines for different C_o. The slopes of these lines represent the apparent rate constants k_{app}. These pseudo-first-order rate constants are inserted in Figure 2 together with their correlation coefficient R^2, which is always greater than 0.98. The k_{app} was calculated for the first stage of the photocatalytic reaction. In this stage, the concentration of HA is predominant relative to the by-products. Accordingly, the rate of reaction depends on the HA concentration, not on by-products. Therefore, the simplified form of the LH model (Equation (12)) was used. Consequently, the experimental data are fitted to the pseudo-first-order kinetic model, as shown in Figure 2. It is noticeable that k_{app} for the degradation of HA in the fixed bed reactor is higher than that in the glass beaker reactor, as is shown in Figure 2. This can be attributed to wall effects of the beaker from absorbing or transmitting part of the incident solar UV light, resulting in a lower captured light energy than calculated. The experimental results show that the k_{app} decreases with increasing C_o of HA. This is consistent with what was reported previously by Li *et al.* (2002) for the degradation of HA by a TiO_2 suspension. As the amount of light absorbed by the HA solution was taken into consideration (see Equations (9) and (10)), therefore, this behaviour could be due to the higher number of adsorbed HA molecules (i.e. q_e) at a high HA C_o. These HA molecules may block some active sites on the TiO_2 surface, which are responsible for the production of active radicals. Hence, the number of produced $^{\bullet}OH$ decreases with increasing HA C_o, leading to a slower rate of photodegradation. This indicates that availability of $^{\bullet}OH$ is rate-limiting by hindering the reaction of HA with the produced $^{\bullet}OH$.

The k_{app} for the degradation of HA by coated meshes was 3.4 times higher than that over a flat plate at the same absorbed energy, the same projected area, and at the same initial HA concentration of 10 mg·L^{-1}.

The validation of LH kinetics for photodegradation of HA with the glass beaker reactor and with the fixed-bed solar reactor can be done by checking the linearity of the relation of $1/r_0$ versus $1/C_0$. The high correlation coefficients ($R^2 = 0.969$ and 0.998 for small and large meshes, respectively) show that the photocatalytic degradation of HA

using TiO_2 coated over the woven meshes obeyed the LH model. According to this model, the rate of reaction (r) is proportional to the fraction of the catalyst surface that is covered by HA. This gives an indication that HA molecules are first adsorbed onto the photocatalyst surface and then decomposed (i.e., the photocatalytic reaction mainly occurs on the catalyst surface and not in the bulk of the solution), which is consistent with previous studies (Bekbolet *et al.* 2002; Li *et al.* 2002). The actual rate constant (k_r) of the reaction, as obtained from Equation (13), for large coated meshes in the recirculating flow fixed-bed reactor (1.495 mg·kJ^{-1}) was close to that for small coated meshes in the batch system (1.462 mg·kJ^{-1}), which proves that up-scaling was feasible.

CONCLUSIONS

- The adsorption kinetics of HA onto TiO_2 film coated over stainless steel woven meshes obeyed pseudo-first-order adsorption kinetics according to the Freundlich adsorption isotherm.
- The degradation kinetics of HA using small coated meshes in the batch reactor and large coated meshes in the recirculating flow fixed-bed solar reactor obeyed the LH kinetic model.
- Up-scaling of mesh size was possible as was shown by the comparable adsorption and photodegradation kinetics for the two investigated reactor sizes.
- The photocatalytic degradation of HA in a solar reactor with four superimposed stainless steel meshes was 3.4 times faster than the flat-plate reactor. This brought the photocatalytic efficiency of such reactors closer to that of dispersed-phase reactors without the complex separation of the TiO_2 photocatalyst.

ACKNOWLEDGEMENTS

This research work has been carried out via the PhD program (El-Kalliny 2013) within the framework of INNOWATOR project, financed by Agentschap NL, the Organization for Prohibition of Chemical Weapons (OPCW), and Egyptian Cultural Affairs & Missions Sector (the Egyptian Government).

REFERENCES

Bandala, E. R., Gelover, S., Leal, M. T., Arancibia-Bulnes, C., Jimenez, A. & Estrada, C. A. 2002 Solar photocatalytic degradation of Aldrin. *Catalysis Today* **76** (2–4), 189–199.

Bekbolet, M., Suphandag, A. S. & Uyguner, C. S. 2002 An investigation of the photocatalytic efficiencies of TiO_2 powders on the decolourisation of humic acids. *Journal of Photochemistry and Photobiology A: Chemistry* **148** (1–3), 121–128.

Dijkstra, M. F. J., Buwalda, H., De Jong, A. W. F., Michorius, A., Winkelman, J. G. M. & Beenackers, A. A. C. M. 2001 Experimental comparison of three reactor designs for photocatalytic water purification. *Chemical Engineering Science* **56** (2), 547–555.

El-Kalliny, A. S. 2013 *Photocatalytic Oxidation in Drinking Water Treatment Using Hypochlorite and Titanium Dioxide*. PhD thesis, Delft University of Technology, Delft, The Netherlands. doi:10.4233/uuid:d829cb31-f1a7-4fec-a9b3-26987757dfc9, 85-100.

El-Kalliny, A. S., Ahmed, S. F., Rietveld, L. C. & Appel, P. W. 2014 Immobilized photocatalyst on stainless steel woven meshes assuring efficient light distribution in a solar reactor. *Drinking Water Engineering and Science* **7** (1), 41–52.

Feitz, A. J., Boyden, B. H. & Waite, T. D. 2000 Evaluation of two solar pilot scale fixed-bed photocatalytic reactors. *Water Research* **34** (16), 3927–3932.

Fujishima, A., Zhang, X. & Tryk, D. A. 2008 TiO_2 photocatalysis and related surface phenomena. *Surface Science Reports* **63** (12), 515–582.

Goetz, V., Cambon, J. P., Sacco, D. & Plantard, G. 2009 Modeling aqueous heterogeneous photocatalytic degradation of organic pollutants with immobilized TiO_2. *Chemical Engineering and Processing: Process Intensification* **48** (1), 532–537.

Kumar, K. V., Porkodi, K. & Rocha, F. 2008 Langmuir–Hinshelwood kinetics – a theoretical study. *Catalysis Communications* **9** (1), 82–84.

Li, X. Z., Fan, C. M. & Sun, Y. P. 2002 Enhancement of photocatalytic oxidation of humic acid in TiO_2 suspensions by increasing cation strength. *Chemosphere* **48** (4), 453–460.

Malato, S., Blanco, J., Richter, C., Milow, B. & Maldonado, M. I. 1999 Solar photocatalytic mineralization of commercial pesticides: methamidophos. *Chemosphere* **38** (5), 1145–1156.

Malato, S., Fernández-Ibáñez, P., Maldonado, M. I., Blanco, J. & Gernjak, W. 2009 Decontamination and disinfection of water by solar photocatalysis: recent overview and trends. *Catalysis Today* **147** (1), 1–59.

McCullagh, C., Skillen, N., Adams, M. & Robertson, P. K. J. 2011 Photocatalytic reactors for environmental remediation: a

review. *Journal of Chemical Technology and Biotechnology* **86** (8), 1002–1017.

Parra, S., Stanca, S. E., Guasaquillo, I. & Thampi, K. R. 2004 Photocatalytic degradation of atrazine using suspended and supported TiO_2. *Applied Catalysis B: Environmental* **51** (2), 107–116.

Qiu, H., Lv, L., Pan, B.-c., Zhang, Q.-j., Zhang, W.-m. & Zhang, Q.-x. 2009 Critical review in adsorption kinetic models. *Journal of Zhejiang University – Science A* **10** (5), 716–724.

Sichel, C., Tello, J., de Cara, M. & Fernández-Ibáñez, P. 2007 Effect of UV solar intensity and dose on the photocatalytic disinfection of bacteria and fungi. *Catalysis Today* **129** (1–2), 152–160.

Yanagida, S., Nakajima, A., Kameshima, Y. & Okada, K. 2006 Effect of applying voltage on photocatalytic destruction of 1,4-dioxane in aqueous system. *Catalysis Communications* **7** (12), 1042–1046.

Zhang, Z., Anderson, W. A. & Moo-Young, M. 2004 Experimental analysis of a corrugated plate photocatalytic reactor. *Chemical Engineering Journal* **99** (2), 145–152.

Zhang, W., Li, Y., Wu, Q. & Hu, H. 2012 Removal of endocrine-disrupting compounds, estrogenic activity, and *Escherichia coliform* from secondary effluents in a TiO_2-coated photocatalytic reactor. *Environmental Engineering Science* **29** (3), 195–201.

Zhao, X., Jia, Q., Song, N., Zhou, W. & Li, Y. 2010 Adsorption of Pb(II) from an aqueous solution by titanium dioxide/carbon nanotube nanocomposites: kinetics, thermodynamics, and isotherms. *Journal of Chemical & Engineering Data* **55** (10), 4428–4433.

First received 11 October 2018; accepted in revised form 25 February 2019. Available online 28 March 2019